First published January 30, 2015; doi:10.1152/ajpheart.00001.2015.

Middle cerebral artery remodeling following transient brain ischemia is linked to early postischemic hyperemia: A target of uric acid treatment

Yara Onetti,[1] Ana P. Dantas,[2] Belén Pérez,[1] Roger Cugota,[1] Angel Chamorro,[3] Anna M. Planas,[4] Elisabet Vila,[1]* and Francesc Jiménez-Altayó[1]*

[1]*Facultat de Medicina, Departament de Farmacologia, Terapèutica i Toxicologia, Institut de Neurociències, Universitat Autònoma de Barcelona, Bellaterra, Spain;* [2]*Institut Clínic del Tòrax, Institut d'Investigacions Biomèdiques August Pi i Sunyer, Barcelona, Spain;* [3]*Functional Unit of Cerebrovascular Diseases, Hospital Clínic de Barcelona, Institut d'Investigacions Biomèdiques August Pi i Sunyer, Barcelona, Spain; and* [4]*Departament d'Isquèmia Cerebral i Neurodegeneració, Institut de Recerca Biomèdica, Consejo Superior de Investigaciones Científicas, Institut d'Investigacions Biomèdiques August Pi i Sunyer, Barcelona, Spain*

Submitted 2 January 2015; accepted in final form 28 January 2015

Onetti Y, Dantas AP, Pérez B, Cugota R, Chamorro A, Planas AM, Vila E, Jiménez-Altayó F. Middle cerebral artery remodeling following transient brain ischemia is linked to early postischemic hyperemia: A target of uric acid treatment. *Am J Physiol Heart Circ Physiol* 308: H862–H874, 2015. First published January 30, 2015; doi:10.1152/ajpheart.00001.2015.—Ischemia impairs blood supply to the brain, and reperfusion is important to restore cerebral blood flow (CBF) and rescue neurons from cell death. However, reperfusion can induce CBF values exceeding the basal values before ischemia. This hyperemic effect has been associated with a worse ischemic brain damage, albeit the mechanisms that contribute to infarct expansion are not clear. In this study, we investigated the influence of early postischemic hyperemia on brain damage and middle cerebral artery (MCA) properties and the effect of treatment with the endogenous antioxidant uric acid (UA). The MCA was occluded for 90 min followed by 24 h reperfusion in adult male Sprague-Dawley rats. Cortical CBF increases at reperfusion beyond 20% of basal values were taken as indicative of hyperemia. UA (16 mg/kg) or vehicle (Locke's buffer) was administered intravenously 135 min after MCA occlusion. Hyperemic compared with nonhyperemic rats showed MCA wall thickening (sham: 22.4 ± 0.8 μm; nonhyperemic: 23.1 ± 1.2 μm; hyperemic: 27.8 ± 0.9 at 60 mmHg; $P < 0.001$, hyperemic vs. sham) involving adventitial cell proliferation, increased oxidative stress, and interleukin-18, and more severe brain damage. Thus MCA remodeling after ischemia-reperfusion takes place under vascular oxidative and inflammatory stress conditions linked to hyperemia. UA administration attenuated MCA wall thickening, induced passive lumen expansion, and reduced brain damage in hyperemic rats, although it did not increase brain UA concentration. We conclude that hyperemia at reperfusion following brain ischemia induces vascular damage that can be attenuated by administration of the endogenous antioxidant UA.

ischemia-reperfusion; oxidative stress; peroxynitrite; interleukin-18; macrophages

REPERFUSION AFTER BRAIN ISCHEMIA is important to restore the blood supply to the brain tissue. Thrombolysis with recombinant tissue plasminogen activator (rtPA) is currently the only approved treatment for ischemic stroke but carries some risks such as hemorrhagic transformation (38). Reperfusion injury is a complex phenomenon attributed to multiple damaging processes, and it could be an important target in stroke therapy. Following experimental brain ischemia, reperfusion can induce cerebral blood flow (CBF) increases above basal levels (33, 34, 35), a process called reactive hyperemia. Reactive hyperemia is not restricted to animals, since there is evidence that some patients can develop hyperperfusion shortly after thrombolysis with rtPA (16). Hyperemia at reperfusion was associated with the worst brain injury in pioneer studies of experimental brain ischemia (33). In a more recent study, rats that developed cortical hyperemia immediately after reperfusion showed larger cortical infarcts and worse neurological deficits than rats not showing hyperemia (23). Therefore, it is suggested that reactive hyperemia at early reperfusion could be a sign of reperfusion injury and also a potential target for therapeutic intervention.

During cerebral ischemia, and particularly at reperfusion, there is a surge of oxidative stress in the brain (29). Certain antioxidants have shown protective effects in preclinical studies of ischemia-reperfusion (I/R), indicating a key role for oxidative stress in brain injury after I/R (27). NO can react with superoxide anion ($O_2^{\cdot -}$) generated at reperfusion to form the potentially harmful molecule peroxynitrite ($ONOO^-$), leading to tissue damage (4). Hyperemic rats show comparatively more brain protein nitrotyrosination that may contribute to the worse outcome (23).

Uric acid (UA) is a powerful endogenous antioxidant that has shown protective effects against ischemic brain damage (1). Several studies provided evidence that exogenously administered UA is neuroprotective in animal models of transient focal brain ischemia (18, 28, 39). The observed neuroprotective effects of UA have led to a multicentric Phase III clinical trial (URICO-ICTUS) to analyze if UA administration increases the clinical benefits of rtPA (1, 5). However, the mechanisms underlying UA-induced neuroprotection are still not completely understood. To date, the mechanisms known to be associated with UA actions following cerebral I/R involve suppression of both reactive oxygen species (ROS) accumulation and lipid peroxidation in the brain (39). Nevertheless, the potential impact of UA effects on the cerebral vasculature after stroke has not been investigated.

Large cerebral arteries, like the middle cerebral artery (MCA), have a strong contribution to total cerebrovascular resistance (10). CBF is tightly controlled by myogenic mechanisms to maintain cerebral perfusion (20). A decrease in MCA myogenic response has been consistently reported after transient MCA occlusion and may contribute to the impaired brain

* E. Vila and F. Jiménez-Altayó contributed equally to this work.

Address for reprint requests and other correspondence: F. Jiménez-Altayó, Departament de Farmacologia, Terapèutica i Toxicología, Facultat de Medicina, Universitat Autònoma de Barcelona, 08193 Bellaterra (Cerdanyola del Vallès), Spain (e-mail: francesc.jimenez@uab.cat).

autoregulation (22). Structural alterations of cerebral arteries may also participate in the development of brain injury (24). Thus, these changes might affect regional CBF regulation and lead to distal capillary destabilization and organ damage. For instance, hypertension, which is a leading cause of stroke, induces remodeling of cerebral arteries causing larger infarcts (15, 24). Several lines of evidence suggest that transient MCA occlusion in rats induces MCA wall thickening (7, 14, 15). Increased oxidative stress seems to be involved in such arterial remodeling since antioxidant treatment at reperfusion rescues MCA from remodeling and reduces infarct volume (14). After cerebral I/R, the inflammatory response is accompanied by an increase in macrophage infiltration (32). In addition, recent reports showed that perivascular macrophage-mediated inflammation could be involved in hypertensive cerebrovascular remodeling (25, 26). Remarkably, the factors underlying MCA remodeling after transient cerebral ischemia are not fully identified.

The present study aims to explore the mechanisms underlying why hyperemia at reperfusion is associated with a worse brain injury after ischemic stroke and the potential beneficial effects of UA antioxidant treatment. We provide the first evidence that postischemic hyperemia is accompanied with a profound vascular oxidative and inflammatory response that contributes to the development of structural alterations in cerebral arteries. Furthermore, we demonstrate that cerebrovascular remodeling is a target of UA treatment, unveiling a potential new mechanism underlying the protective effects of this compound.

MATERIALS AND METHODS

Animals. Seventy-seven adult male Sprague-Dawley rats obtained from Harlan (Barcelona, Spain) were housed under a 12:12-h light-dark cycle, controlled environmental conditions of temperature and humidity, and provided with access to food and water ad libitum. All of the experiments were carried out under the Guidelines established by the Spanish legislation (RD 1201/2005) and according to the *Guide for the Care and Use of Laboratory Animals*, published by the United States National Institutes of Health (NIH Publication 85-23, revised 1996). Experiments were approved by the Ethics Committee of the Universitat Autònoma de Barcelona and were carried out in compliance with the European legislation.

Experimental cerebral ischemia. The surgical procedure for induction of focal cerebral ischemia was previously described (23). Rats were anesthetized with isoflurane (2.5–3%) vaporized in O_2 and N_2O (30:70). Mean femoral arterial blood pressure was monitored, and body temperature was maintained between 37.0 and 37.5°C during surgery. Briefly, the common and external carotid arteries were exposed, and the pterygopalatine artery was ligated. A filament (nylon monofilament 4/0; Suturas Aragó, Barcelona, Spain) heat rounded at the tip was introduced (21 mm) through the internal carotid artery to the level where the MCA branches out, and a ligature was placed on the internal carotid artery. The filament was cautiously removed to allow reperfusion following 90 min of occlusion. Sham-operated animals were also carried out by performing the full surgical procedure and by introducing the filament through the MCA for <1 min. A simple neurological test on a nine-point scale (0 = no deficit to 9 = highest handicap) was performed before killing the animals, as reported (23). At 24 h, rats were killed under deep isoflurane anesthesia, and the brain was removed and placed in cold Krebs-Henseleit solution (KHS) (14, 15). Evaluation of infarct volume was performed with the 2,3,5-triphenyltetrazolium chloride (Sigma-Aldrich, St. Louis, MO) technique, as described (23).

Measurement of CBF. Changes in cortical CBF were measured with a laser-Doppler system (Perimed, Järfalla, Sweden), as reported (23). CBF was continuously monitored for 30 min before ischemia, during the ischemia period, and during the first hour after reperfusion. Values of cortical CBF after reperfusion (during the first 15 min) that recovered to their corresponding baseline values (before occlusion) (≤20%) were considered normoperfused (nonhyperemic), whereas increases of cortical CBF above 20% of basal values were considered hyperperfused and a sign of reactive hyperemia (23). Subarachnoid hemorrhage ($n = 5$) or unsuccessful blood flow measurements because of technical surgical problems ($n = 6$) were used as criteria to exclude animals from the study.

Treatment. One hundred and thirty-five minutes after the onset of ischemia (i.e., after 45 min of reperfusion), rats were treated with either UA (16 mg/kg) or vehicle (Locke's buffer) intravenously infused during 20 min. The dose used was previously shown to protect against damage induced by transient focal ischemic brain injury (18, 28, 39).

Animals were randomly assigned to sham operation or ischemia. Ischemic animals were divided into two groups depending on whether they developed hyperemia at reperfusion. Finally, sham-operated, nonhyperemic-ischemic, and hyperemic-ischemic groups received either UA or vehicle as follows: sham-operated vehicle (sham + VEH, $n = 13$); ischemic nonhyperemic vehicle (I/NH + VEH, $n = 11$); ischemic hyperemic vehicle (I/H + VEH, $n = 12$); sham-operated treated with UA (sham + UA, $n = 5$); ischemic nonhyperemic UA (I/NH + UA, $n = 8$); and ischemic hyperemic UA (I/H + UA, $n = 12$).

Tissue preparation. The MCA from the right (ipsilateral to ischemia) and left (contralateral to ischemia) hemisphere was dissected under a surgical microscope and kept in cold KHS. The proximal segment of the ipsilateral MCA was immediately used for pressure myography and processed for nuclei distribution microscopic fluorescence studies (15). Distal ipsilateral MCA segments were used for evaluation of $O_2^{\cdot-}$ production, immunofluorescence, and mRNA levels (14). Coronal brain sections for immunofluorescence studies were processed as described (23). Plasma (500 μl) was collected intracardially just before rats were killed and was kept at −70°C until the day of nitrite level and multiple ELISA studies. A separate group of rats was used for the analysis of UA levels in plasma and brain by high-performance liquid chromatography (HPLC).

Parallel artificial membrane permeation assay for blood-brain barrier. To evaluate the predictive penetration of UA by passive transport to the brain, parallel artificial membrane permeation assay for blood-brain barrier (PAMPA-BBB) was used following the method described by Di et al. (9). The in vitro permeability (P_e) of 14 commercial drugs through lipid extract of porcine brain membrane together with the test compounds was determined (3 different experiments in triplicate). A lineal correlation between experimental and reported (9) permeability of selected commercial drugs using the PAMPA assay was evaluated ($y = 1.566x - 1.089$; $R^2 = 0.9303$) to validate the assay. From this equation and taking into account the limits established by Di et al. (9) for BBB permeation, we established the ranges of permeability as compounds of high BBB permeation [central nervous system $(CNS)^+$]: P_e (10^{-6} cm/s) >5.175; compounds of low BBB permeation (CNS^-): P_e (10^{-6} cm/s) <2.043; and compounds of uncertain BBB permeation ($CNS^{+/-}$): $5.175 > P_e$ (10^{-6} cm/s) > 2.043.

Determination of UA levels in plasma and brain. The concentration of UA in plasma and brain tissue was evaluated by HPLC with ultraviolet detection. Blood samples were obtained from vehicle- and UA-treated animals at different time points (ranging from 10 min to 24 h) under isoflurane anesthesia. Animals were anesthetized and perfused through the heart with saline to remove blood from brain vessels. The brain was obtained 10 and 30 min after UA administration. The method used for UA extraction was adapted from a method

previously described (17). Briefly, plasma (100 μl) and brain tissue (700 mg) were deproteinized with 10% TCA (20 μl plasma/150 μl brain). Samples were sonicated for 20 s and centrifuged (5 min; 12,000 *g*). Afterwards, 10 μl supernatant were injected into the HPLC system (PerkinElmer, Madrid, Spain) made of a 200 Pump, a 717 plus Auto sampler, and a 2487 Dual λ absorbance detector. A reverse-phase ODS2 (4.6·200 mm, 5-μm particle size; Waters, Barcelona, Spain) was used. The mobile phase was methanol-5 mM ammonium acetate-acetonitrile (1:96:3 vol/vol/vol), which was run with an isocratic regular low flow rate of 1.2 ml/min, and the wavelength ultraviolet detector was set at 292 nm. Quantification was performed by external calibration. The UA peak in plasma and brain was confirmed by mass spectrometry.

Nitrite levels. NO production was determined by measuring the plasma nitrite contents with the Griess reagent (11). The absorbance at 540 nm was measured, and the nitrite concentration was determined by using a calibration curve of standard sodium nitrite concentrations vs. absorbance.

Pressure myography. The structural, mechanical, and myogenic properties of the MCA were studied with a pressure myograph (Danish Myo Tech model P100; J.P. Trading, Aarhus, Denmark), as described previously (14, 15). In brief, the vessel was placed on two glass microcannulas and secured with surgical nylon suture. Intraluminal pressure was reduced to 3 mmHg, and a pressure-diameter curve (3–120 mmHg) was obtained in gassed KHS (37°C). Internal and external diameters (D_{iCa}, D_{eCa}) were measured for 3 min at each intraluminal pressure. The artery was then set to 70 mmHg and allowed to equilibrate for 30 min at 37°C in gassed calcium-free KHS (0 Ca^{2+}: omitting calcium and adding 10 mM EGTA). A second pressure-diameter curve was obtained in 0 Ca^{2+} KHS, and D_{i0Ca} and D_{e0Ca} were measured. Structural, mechanical, and myogenic parameters were analyzed as previously described (14, 15).

Measurement of $O_2^{\cdot-}$ production. The oxidative fluorescent dye dihydroethidium was used to evaluate production of MCA $O_2^{\cdot-}$ in situ, as described previously (14). The specificity of the signal for $O_2^{\cdot-}$ was evaluated by incubation with the $O_2^{\cdot-}$ scavenger Mn(III)tetrakis(1-methyl-4-pyridyl)porphyrin (0.1434 mg/ml, 30 min, 37°C) (Sigma-Aldrich). Under the latter condition, no hydroethidine (HE) fluorescence was observed in the tissue in any experimental situation. Quantitative analysis of HE fluorescence was performed with MetaMorph Image Analysis software (Molecular Devices, Sunnyvale, CA), as reported (14, 23).

Immunofluorescence. Frozen transverse sections (14 μm thick) of MCA or coronal brain sections (50 μm thick) were incubated (1 h) with a mouse monoclonal antibody against eNOS (1:100; BD Biosciences, Franklin Lakes, NJ) and cluster of differentiation 68 (CD68, 1:75; AbD Serotec, Kidlington, Oxford, UK); a rabbit polyclonal antibody against interleukin (IL)-18 (1:50; Santa Cruz Biotechnology, Santa Cruz, CA), nitrotyrosine (1:100; Merck Millipore, Billerica, MA), iNOS (1:50; Thermo Scientific, Rockford, IL), and nNOS (1:100; Life Technologies, Alcobendas, Spain); a rabbit monoclonal antibody against phosphorylated extracellular signal-regulated kinase 1/2 (pERK1/2, 1:100; Cell Signaling Technology, Danvers, MA); or a goat polyclonal antibody against vascular cell adhesion molecule-1 (VCAM-1; 1:50, Santa Cruz Biotechnology). After being washed, sections were incubated (45 min) with the secondary antibodies (1:200), a donkey anti-mouse, anti-rabbit, or anti-goat IgG conjugated to Cyanine 3 (Jackson ImmunoResearch Laboratories, West Grove, PA) or Alexa Fluor 568 (Life Technologies) at 37°C. Sections were processed for immunofluorescence staining essentially as previously described (14, 23). The specificity of the immunostaining was verified by omission of the primary antibody and processed as above, which abolished the fluorescence signal. Quantification of CD68-positive cells ($CD68^+$) was performed in a systematic manner, and the count average per ring was calculated for each rat. Quantitative analysis of fluorescence was performed with MetaMorph Image Analysis software (Molecular Devices) as reported (14). In brain, a similar subcortical area from the ipsilateral hemisphere was selected for each experimental condition (coinciding with the infarcted area in ischemic groups), and the complete image field fluorescence (750 × 750 μm) was analyzed. The results were expressed as arbitrary units.

Nuclei distribution by confocal microscopy. Pressure (70 mmHg)-fixed intact MCA was stained with the nuclear dye Hoechst 33342 (10 μg/ml) for 30 min (15). After washing was completed, arteries were mounted on slides with a well made of silicon spacers to avoid artery deformation. They were visualized with a Leica TCS SP2 (Heidelberg, Germany) confocal system. Stacks of serial optical slices (0.5 μm thick) were captured from the adventitia to the lumen of each artery. The different MCA layers stained with Hoechst 33342 were clearly distinguished with confocal microscopy according to the shape and/or orientation of the cell nuclei (2). At least, two stacks of images of several regions were captured in each arterial segment. MetaMorph Image Analysis software (Molecular Devices) was used for quantification. The nuclei number was counted in the *z*-axis, as previously described (15).

Multiple ELISA. Plasma samples were prepared for analysis in a 96-well plate using a custom 27-cytokine Milliplex MAP Rat Cytokine/Chemokine Magnetic Bead Panel (RECYMAG65K27PMX; Millipore) following the kit-specific protocols. Analytes were quantified using a Magpix analytical test instrument that uses xMAP technology (Luminex, Austin, TX) and xPONENT 4.2 software (Luminex).

Quantitative real-time PCR. mRNA expression was quantified by Syber green-based quantitative real-time PCR (qRT-PCR) as previously described (21). The expression of mRNA for GAPDH of 18S ribosomal RNA was used as an internal control. qRT-PCR reactions were set following the manufacturer's conditions. C_t values obtained for each gene were referenced to GAPDH 18S ($\Delta\Delta C_t$) and converted to the linear form using the term $2^{-\Delta\Delta C_t}$ as a value directly proportional to the copy number of cDNA and initial quantity of mRNA (21).

Statistics. Results were expressed as means ± SE of the number (*n*) of rats indicated in the legends for Figs. 1–9. The difference between nonhyperemic or hyperemic rats and the effect of UA treatment were assessed by a two-way ANOVA with Bonferroni's posttest to compare groups. Data analysis was carried out using GraphPad Prism version 4 software. A value of $P < 0.05$ was considered significant.

RESULTS

Body weight, mean arterial blood pressure, and body temperature during surgery did not vary between groups (Table 1). None of the rats died in either group before the end of the study. The incidence of reactive hyperemia was 56%. The reduction of CBF during ischemia was similar in all the groups, and the extent of CBF increase at reperfusion in the hyperemic groups that later received either UA or vehicle was not different (Table 2).

UA treatment is neuroprotective in animals showing reactive hyperemia. Larger infarct volumes in cortical and subcortical regions were observed in rats showing reactive hyperemia at reperfusion compared with those that did not develop hyperemia (Fig. 1*A*). Single-dose administration of UA at 135 min after the onset of ischemia reduced ($P < 0.05$) infarct volume in hyperemic, but not in nonhyperemic, rats (Fig. 1*A*). Likewise, the neurological score was worse ($P < 0.001$) in hyperemic than in nonhyperemic animals (Fig. 1*B*). Treatment with UA ameliorated ($P < 0.01$) the neuro-

Table 1. *Body weight and physiological parameters at different time points during anesthesia and surgery*

	I/NH		I/H	
	Vehicle	Uric acid	Vehicle	Uric acid
Body wt, g	275.90 ± 5.75	264.86 ± 3.96	260.39 ± 4.96	260.25 ± 4.46
Mean arterial blood pressure, mmHg				
Before ischemia	93.64 ± 1.31	91.86 ± 1.57	92.67 ± 2.43	92.20 ± 2.92
During ischemia (60 min)	93.50 ± 1.11	93.00 ± 1.45	92.00 ± 2.25	90.80 ± 2.33
Immediately after reperfusion	91.83 ± 1.09	90.57 ± 1.36	92.34 ± 2.17	92.00 ± 2.63
Body temperature, °C				
Before ischemia	37.24 ± 0.13	36.85 ± 0.21	37.59 ± 0.13	37.38 ± 0.18
During ischemia (60 min)	37.46 ± 0.15	37.26 ± 0.14	36.97 ± 0.10	37.21 ± 0.09
Immediately after reperfusion	37.20 ± 0.12	36.80 ± 0.13	37.31 ± 0.16	36.98 ± 0.10

Results are means ± SE from ischemic/nonhyperemic (I/NH; vehicle: $n = 11$; uric acid: $n = 8$) and ischemic/hyperemic (I/H); vehicle: $n = 12$; uric acid: $n = 12$) rats.

logical score in hyperemic rats without modifying it in nonhyperemic rats (Fig. 1*B*).

MCA structural alterations are associated with reactive hyperemia and are prevented by UA treatment. Arterial diameters were measured over the pressure range from 3 to 120 mmHg under fully relaxed conditions (0 Ca^{2+}-KHS), and the influence of hyperemia and in vivo UA treatment on the MCA structural properties was studied. Twenty four hours following I/R, the MCA from rats not manifesting reactive hyperemia (nonhyperemic) did not display alterations in external and lumen diameters compared with the MCA of sham-operated rats (Fig. 2, *A* and *B*). Conversely, hyperemia was associated with enlarged ($P < 0.05$) external diameters compared with sham-operated rats (Fig. 2*A*). Administration of UA did not significantly alter external diameters but caused a lumen diameter increase ($P < 0.05$) in hyperemic rats and a trend to increase ($P = 0.06$) in nonhyperemic rats compared with the sham group (Fig. 2, *A* and *B*). After I/R, the MCA wall of nonhyperemic rats was not structurally different from that of sham-operated rats (Fig. 2, *C* and *D*). In contrast, enlarged wall thickness (Fig. 2*C*) and cross-sectional area (Fig. 2*D*), but not wall/lumen (results not shown), were found in hyperemic rats compared with the sham group. Of note, the vehicle (Locke's buffer) had no effect on MCA structure, since nontreated hyperemic rats displayed the same remodeling observed in hyperemic rats that received the vehicle (data not shown). Notably, UA treatment prevented all hyperemia-induced MCA structural alterations and did not affect MCA structure in sham rats (Fig. 2, *C* and *D*).

Analysis of the passive mechanical properties showed that hyperemia decreased wall stress ($P < 0.05$), and UA treatment prevented this effect (Fig. 3*A*). The stress-strain relationship (Fig. 3*B*) and the β-values of the stress-strain relationship were similar irrespective of I/R (sham + VEH: 6.9 ± 0.3, $n = 13$; I/NH + VEH: 6.7 ± 0.2, $n = 11$; I/H + VEH: 7.5 ± 0.5, $n = 12$) and treatment (sham + UA: 6.5 ± 0.1, $n = 5$; I/NH + UA: 5.8 ± 0.4, $n = 8$; I/H + UA: 6.5 ± 0.3, $n = 12$), indicating that the vessel stiffness was not significantly altered by I/R or treatment.

Table 2. *Percentage changes in cortical CBF during ischemia (90 min) and reperfusion (first 15 min) with respect to basal values*

	I/NH		I/H	
Basal CBF, %	Vehicle	Uric acid	Vehicle	Uric acid
Ischemia	46.2 ± 3.7	44.7 ± 3.9	37.1 ± 3.7	46.6 ± 4.7
Reperfusion	88.1 ± 6.2	93.1 ± 2.2	138.9 ± 5.5***	130.0 ± 2.8***

Results are means ± SE from I/NH (vehicle: $n = 11$; uric acid: $n = 8$) and I/H (vehicle: $n = 12$; uric acid: $n = 12$) rats. CBF, cerebral blood flow. ***$P < 0.001$, I/H vehicle vs. I/NH vehicle or I/H uric acid vs. I/NH uric acid by 2-way ANOVA with Bonferroni's posttest.

Ischemia-induced MCA myogenic alterations are not related to reactive hyperemia and are unaffected by UA treatment. Lumen diameter in active conditions (2.5 mM Ca^{2+}-KHS) was significantly enlarged ($P < 0.05$) over the pressure range after I/R, irrespective of the presence or absence of hyperemia, and UA did not modify it (Fig. 3*C*). Internal diameter reductions in active relative to passive (0 Ca^{2+}-KHS) conditions reveal the extent of the constrictor tone and reflect the myogenic response as a function of pressure (Fig. 3*D*). Ischemia, regardless of hyperemia, decreased ($P < 0.05$) the myogenic response, and UA was not able to prevent this response (Fig. 3*D*). However, analysis of slopes of the myogenic response-pressure curves (myogenic reactivity) showed that this parameter was not modified either by I/R (sham + VEH: 0.05 ± 0.05, $n = 13$; I/NH + VEH: −0.01 ± 0.03, $n = 11$; I/H + VEH: 0.05 ± 0.04, $n = 12$) or treatment (sham + UA: 0.02 ± 0.06, $n = 5$; I/NH + UA: 0.01 ± 0.05, $n = 8$; I/H + UA: 0.01 ± 0.03, $n = 12$).

UA suppresses the hyperemia-induced increase in both adventitial volume and AC proliferation. Nuclei distribution measurements by confocal microscopy from intact and pressurized MCA are reported in Fig. 4*A*. The development of hyperemia was associated with an enlargement of wall and adventitial volume in relation to sham-operated rats, coupled with a higher number of both ACs and smooth muscle cells (SMCs) in the MCA wall with no changes in media volume. This effect was not observed in ischemic rats that did not develop hyperemia. UA treatment prevented the increased wall and adventitial volume and the augmented number of ACs, but not SMCs, in the hyperemic group. Cell proliferation in the MCA wall was further supported by the increased expression of pERK1/2, a key intracellular signal for stimuli-induced cell proliferation, along the MCA wall of hyperemic rats, which was reduced by UA treatment (Fig. 4*B*).

Increased cerebrovascular oxidative stress is reduced by UA treatment. We evaluated HE fluorescence along the arterial wall to assess for $O_2^{\cdot -}$ production. HE fluorescence along the ipsilateral MCA wall was increased ($P < 0.05$) in both non-

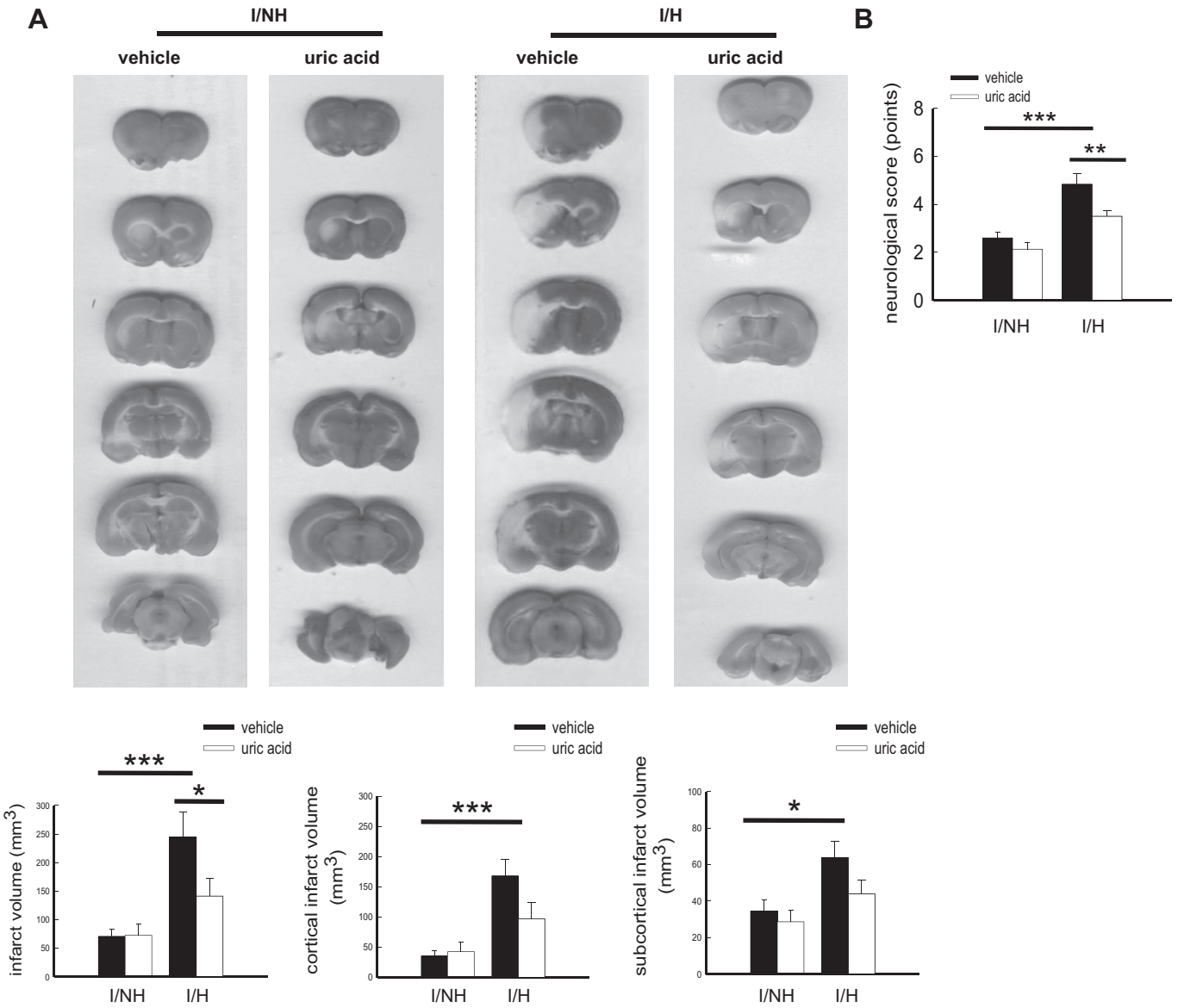

Fig. 1. Beneficial effect of uric acid after ischemia (90 min)-reperfusion (24 h). Rats received the vehicle or uric acid at 135 min after the onset of ischemia. *A*: representative images of coronal brain sections stained with 2,3,5-triphenyltetrazolium chloride and quantification (*bottom*) of infarct volume. *B*: effects of uric acid on neurological score. I/NH, ischemic/nonhyperemic; I/H, ischemic/hyperemic. Results are means ± SE from I/NH (vehicle: $n = 11$; uric acid: $n = 8$) and I/H (vehicle: $n = 12$; uric acid: $n = 12$) rats. *$P < 0.05$, **$P < 0.01$, and ***$P < 0.001$ by 2-way ANOVA.

hyperemic and hyperemic rats compared with sham-operated rats (Fig. 5*A*). Conversely, the contralateral MCA did not display elevated HE fluorescence after I/R (results not shown). UA treatment slightly diminished the enhanced HE fluorescence in nonhyperemic rats and reduced ($P < 0.001$) it in hyperemic rats (Fig. 5*A*). Quantitative analysis of mRNA levels of NAD(P)H oxidase subunits (major source of vascular $O_2^{\cdot -}$) showed augmented ($P < 0.05$) gp91^{phox} and p22^{phox} mRNA expression in hyperemic compared with sham-operated rats, and this effect was attenuated ($P < 0.05$) by UA (Fig. 5*A*). However, UA treatment increased p22^{phox} mRNA levels in nonhyperemic rats.

Hyperemia is associated with enhanced protein nitrotyrosination, and UA reduces this effect. The reaction of $O_2^{\cdot -}$ and NO can lead to $ONOO^-$ formation, which can induce irreversible protein nitrotyrosination. Only the MCA from hyperemic rats showed an increase ($P < 0.05$) in nitrotyrosine immunofluorescence vs. that of sham-operated rats, and this effect was particularly prominent in the adventitia (Fig. 5*B*). Similarly, only hyperemic rats showed increased ($P < 0.01$) nitrotyrosine fluorescence in brain tissue (Fig. 6). UA treatment reduced ($P < 0.05$) nitrotyrosine immunofluorescence in both the MCA and the brain tissue of hyperemic rats (Figs. 5*B* and 6). Expression of eNOS, iNOS, and nNOS in the MCA, as assessed by immunofluorescence, was unaltered by I/R compared with sham operation (results not shown). However, plasma nitrite levels (μmol/l) were higher ($P < 0.05$) in hyperemic than in sham-operated rats (sham + VEH: 11.62 ± 0.36, $n = 6$; I/NH + VEH: 11.81 ± 0.97, $n = 7$; I/H + VEH: 13.77 ± 0.68, $n = 5$) and were reduced ($P < 0.05$) by UA treatment (sham + UA: 12.25 ± 0.36, $n = 4$; I/NH + UA: 12.10 ± 0.72, $n = 6$; I/H + UA: 10.87 ± 0.74, $n = 7$).

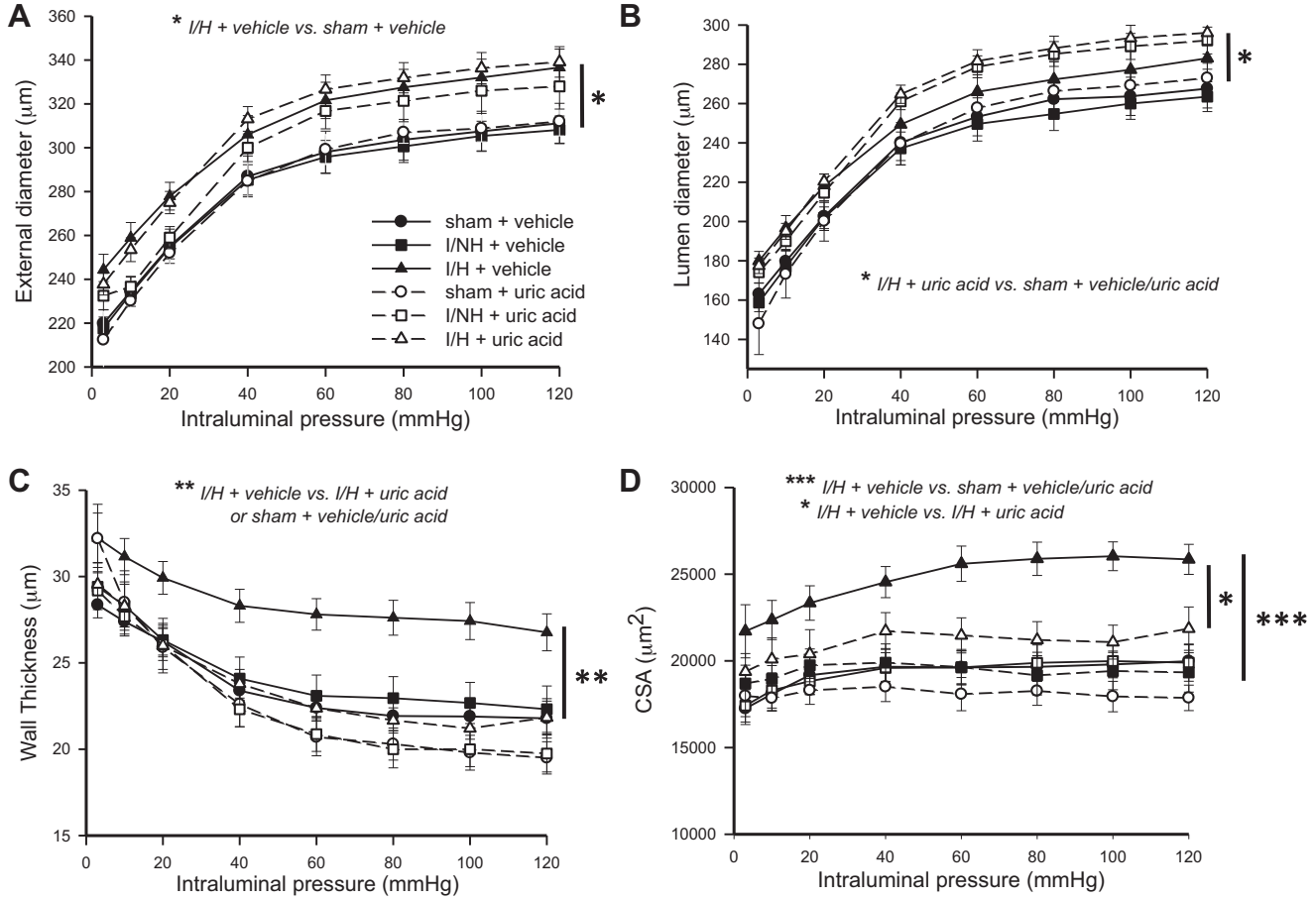

Fig. 2. Influence of uric acid treatment on structural alterations induced by ischemia-reperfusion in rat middle cerebral arteries. External (*A*) and lumen (*B*) diameter in passive conditions [0 Ca^{2+}-Krebs-Henseleit solution (KHS)]. *C* and *D*: wall thickness-intraluminal pressure (*C*) and cross-sectional area (CSA)-intraluminal pressure (*D*) in passive conditions. Results are means ± SE from sham (vehicle: $n = 13$; uric acid: $n = 5$), I/NH (vehicle: $n = 11$; uric acid: $n = 8$), and I/H (vehicle: $n = 12$; uric acid: $n = 12$) rats. $^*P < 0.05$, $^{**}P < 0.01$, and $^{***}P < 0.001$ by 2-way ANOVA.

Elevated levels of circulating IL-1β and IL-18 are a signature of hyperemia and are reduced by UA treatment. To identify potential specific pathways responsible for vascular remodeling in hyperemic animals, we first compared cytokine/chemokine profiling in plasma of sham-operated and I/R rats at 24 h after reperfusion. Among 27 cytokines/chemokines, IL-1β (Fig. 7*A*) and IL-18 (Fig. 7*B*) were the only cytokines showing a statistically significant increased concentration in hyperemic compared with sham-operated rats, whereas they were unchanged in nonhyperemic rats. UA treatment normalized hyperemia-induced increases in both IL-1β and IL-18 circulating levels.

Hyperemia is linked to increased monocyte/macrophage recruitment irrespective of UA treatment. Although we did not detect significant changes in VCAM-1 mRNA expression in the MCA 24 h after I/R, VCAM-1 protein expression along the MCA wall increased, predominantly in the adventitia, regardless of hyperemia or UA treatment (Fig. 8*A*). $CD68^+$ cells were detected in the endothelium and adventitia of the MCA, although they were especially abundant in the latter (Fig. 8*B*). Hyperemic rats showed an increased $CD68^+$ cell count in the MCA wall that was not modified by UA treatment (Fig. 8*B*).

MCA IL-18 levels increase after hyperemia and are reduced by UA treatment. Local IL-18 protein expression in the MCA wall (Fig. 8*B*) was increased ($P < 0.01$) in hyperemic animals, particularly in the endothelium and adventitia. This effect was prevented by UA treatment ($P < 0.05$). Quantitative analysis of IL-18 mRNA levels showed that hyperemia was associated with an increase ($P < 0.05$) in IL-18 mRNA expression in the MCA that again was reduced by UA. Of note, IL-18 mRNA levels were diminished ($P < 0.05$) in nonhyperemic animals compared with sham-operated animals, and increased ($P < 0.05$) after UA treatment. Neither the endogenous neutralizer of IL-18, IL-18-binding protein, nor IL-1β mRNA levels were significantly altered by hyperemia or UA (results not shown).

UA does not penetrate to the brain parenchyma. Table 3 shows permeability results from different commercial compounds and UA using the PAMPA-BBB assay. The assay showed that problem compounds displayed similar experimental permeability values as those reported in the literature, and some of them manifested positive predictive penetration into the CNS. However, UA permeability was poor, which suggests that it does not cross the BBB by passive transport. Plasma and brain UA levels are shown in Fig. 9.

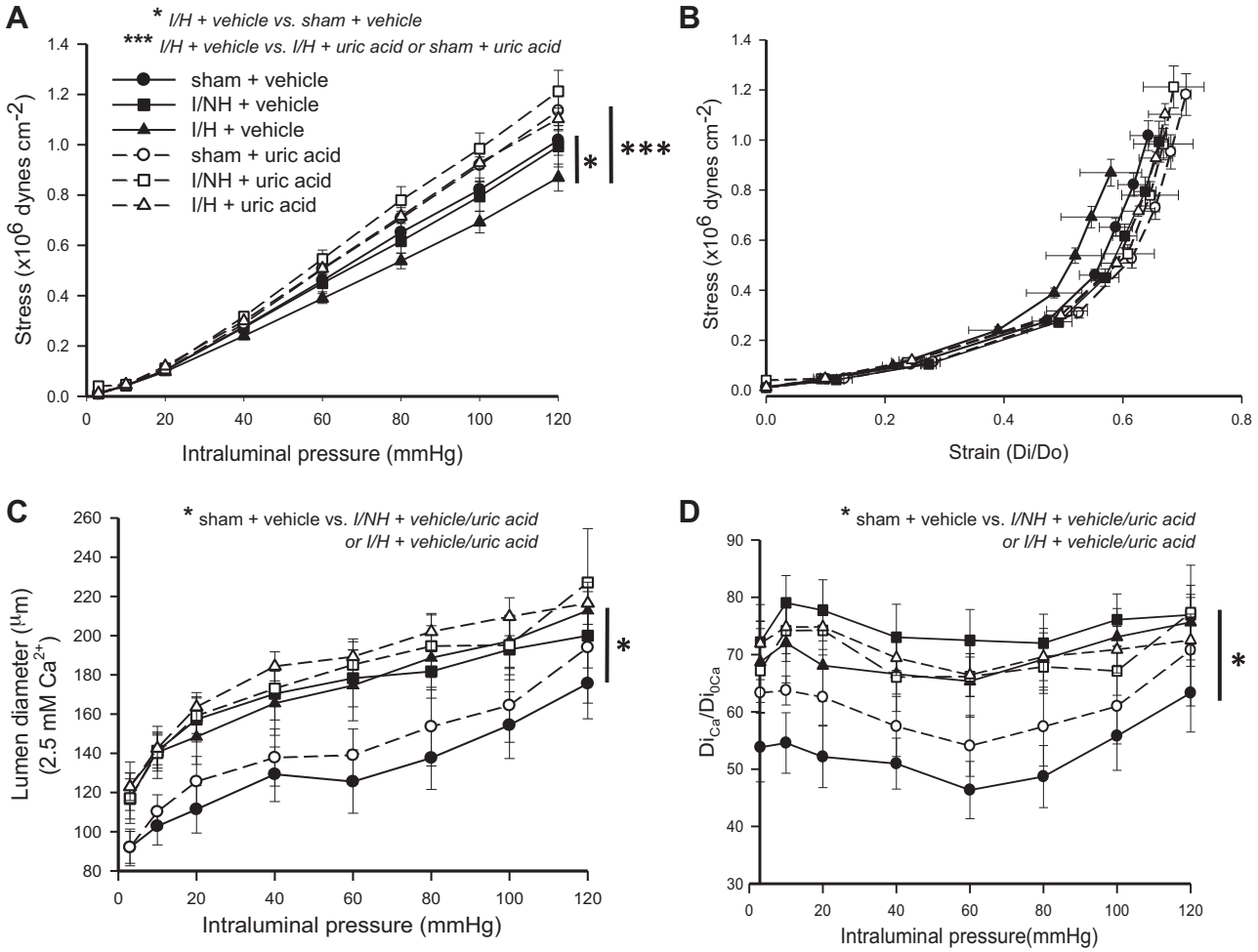

Fig. 3. Influence of ischemia-reperfusion and uric acid treatment on mechanical and myogenic properties of rat middle cerebral arteries. *A*: stress-intraluminal pressure. *B*: stress-strain [observed internal diameter from a given intravascular pressure (D_i)/internal diameter at 3 mmHg (D_o)]. *C*: lumen diameter in active conditions (2.5 mM Ca^{2+}-KHS). *D*: internal diameter in active (D_{iCa}) relative to passive (D_{i0Ca}) conditions. Results are means ± SE from sham (vehicle: n = 13; uric acid: n = 4–5), I/NH (vehicle: n = 11; uric acid: n = 8), and I/H (vehicle: n = 12; uric acid: n = 12) rats. *$P < 0.05$ and ***$P < 0.001$ by 2-way ANOVA.

In either plasma (Fig. 9*B*) or brain (Fig. 9*C*), levels of endogenous UA were similar in both sham and ischemic rats. UA plasma levels increased 10 min after intravenous UA administration and returned to baseline from 10 min onwards (Fig. 9*B*). In contrast, UA levels in brain tissue were unaffected by UA infusion (Fig. 9*C*).

DISCUSSION

UA is a potent endogenous antioxidant with encouraging protective effects in ischemic stroke after exogenous administration (5, 18, 28, 39). To date, only one study reported reduction in infarct volume and improved neurological scores after UA treatment administered in a clinically relevant timeframe (180 min after MCA occlusion) (39). In previous studies, development of hyperemia at reperfusion following an episode of brain ischemia was associated with larger infarcts and worse neurological deficits (23). In the present study, we also found that hyperemic rats show larger infarctions and document that UA, administered 135 min after MCA occlusion, decreases infarct volume and improves the neurological score in rats manifesting hyperemia. Therefore, the results of the current study support that exogenously administered UA is effective in the rats showing signs of reactive hyperemia at reperfusion and further identify the cerebral vasculature as a target of UA protection.

Several reports documented hypertrophy of the MCA after transient MCA occlusion (7, 14, 15), and one study (7) suggested that structural alterations may take place after reperfusion. The results of the present study extend those observations and demonstrate for the first time that only those animals that showed hyperemia at early reperfusion displayed arterial wall hypertrophy, which in turn was associated with larger infarct volumes. Based on those observations, we suggest that MCA wall thickening after I/R can be considered a sign of reperfusion injury. UA prevented the hypertrophic response in the MCA induced by hyperemia, suggesting that protection of cerebrovascular structure is a potential mechanism underlying the beneficial effects of UA. Of note, we found that UA displayed low predictive penetration in the CNS and endogenous brain levels of UA were not modified after UA intravenous infusion, suggesting that the target of this compound could be the brain vasculature.

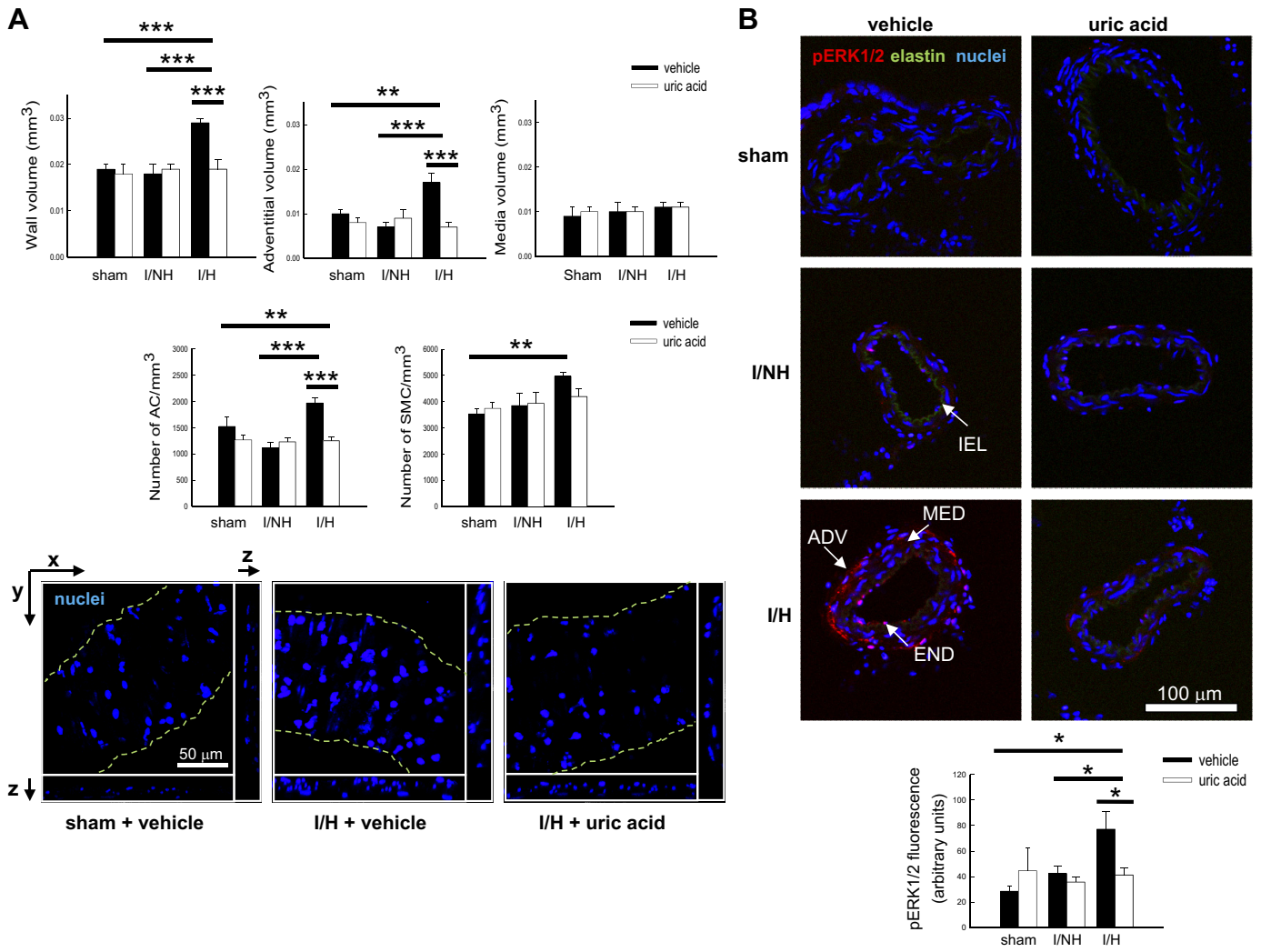

Fig. 4. Influence of uric acid treatment on cellular alterations induced by ischemia-reperfusion in rat middle cerebral arteries. *A*: comparison of morphological parameters in pressurized intact segments of middle cerebral arteries. The arteries were incubated with Hoechst 33342 (10 μg/ml) to stain cell nuclei (blue), and stacks of serial optical slices were taken with a laser scanning confocal microscope. Representative adventitia-level orthogonal reconstructions of confocal Z-stacks (*bottom*) are shown. *B*: representative photomicrographs and quantification of phosphorylated extracellular signal-regulated kinase 1/2 (pERK1/2) immunofluorescence of confocal microscopic artery sections. Immunofluorescence signal (red), natural autofluorescence of elastin (green), and nuclear staining (blue) are shown. AC, adventitial cells; SMC, smooth muscle cells; ADV, adventitial layer; MED, media layer; END, endothelial layer; IEL, internal elastic lamina. Results are means ± SE from sham (vehicle: $n = 4$; uric acid: $n = 3$–5), I/NH (vehicle: $n = 4$; uric acid: $n = 4$), and I/H (vehicle: $n = 3$–4; uric acid: $n = 4$–5) rats. $^*P < 0.05$, $^{**}P < 0.01$, and $^{***}P < 0.001$ by 2-way ANOVA with Bonferroni's posttest.

The reduction of CBF during ischemia was similar in all the groups, indicating that hyperemia was not attributable to a more severe CBF drop during ischemia, in agreement with a previous study (23). However, we cannot exclude that hyperemia might be related to higher reductions of CBF in the core of the infarction during ischemia, since our laser Doppler CBF measurement was taken from a superficial cortical area. Previous studies have proposed that hyperemia is linked to an increase in NO production (12, 13). In the present study we did not find changes in MCA NOS protein expression among groups. However, we cannot exclude an increase in MCA NOS activity in hyperemic animals, since circulating nitrite levels were higher in hyperemic rats, suggesting a surge of NO production. In addition to producing relaxation, NO exerts its protective action by scavenging $O_2^{\cdot -}$. However, the product of this reaction yields the highly reactive molecule $ONOO^-$ that generates protein oxidation and nitrotyrosination (4). The marked protein nitrotyrosination along the MCA wall detected in hyperemic rats extends our previous findings of exacerbated brain protein nitrotyrosination in hyperemic animals (23) and suggests that major nitrotyrosination of the MCA after I/R (8, 14, 19, 22) is associated with reactive hyperemia.

A decrease in the myogenic response is considered an important factor involved in the functional dysregulation of CBF after I/R (22). Previous studies reported a threshold of MCA occlusion for myogenic responses in the rat MCA (6). Consistently, here we show that myogenic alterations do not depend on the degree of blood flow increase at early reperfusion, since both nonhyperemic and hyperemic rats displayed similar myogenic response impairment compared with sham-operated rats. It has been proposed that one of the mechanisms associated with loss of MCA myogenic response is the $ONOO^-$-induced nitrotyrosination and subsequent loss of filamentous actin (8, 19, 22). In our study, the myogenic response

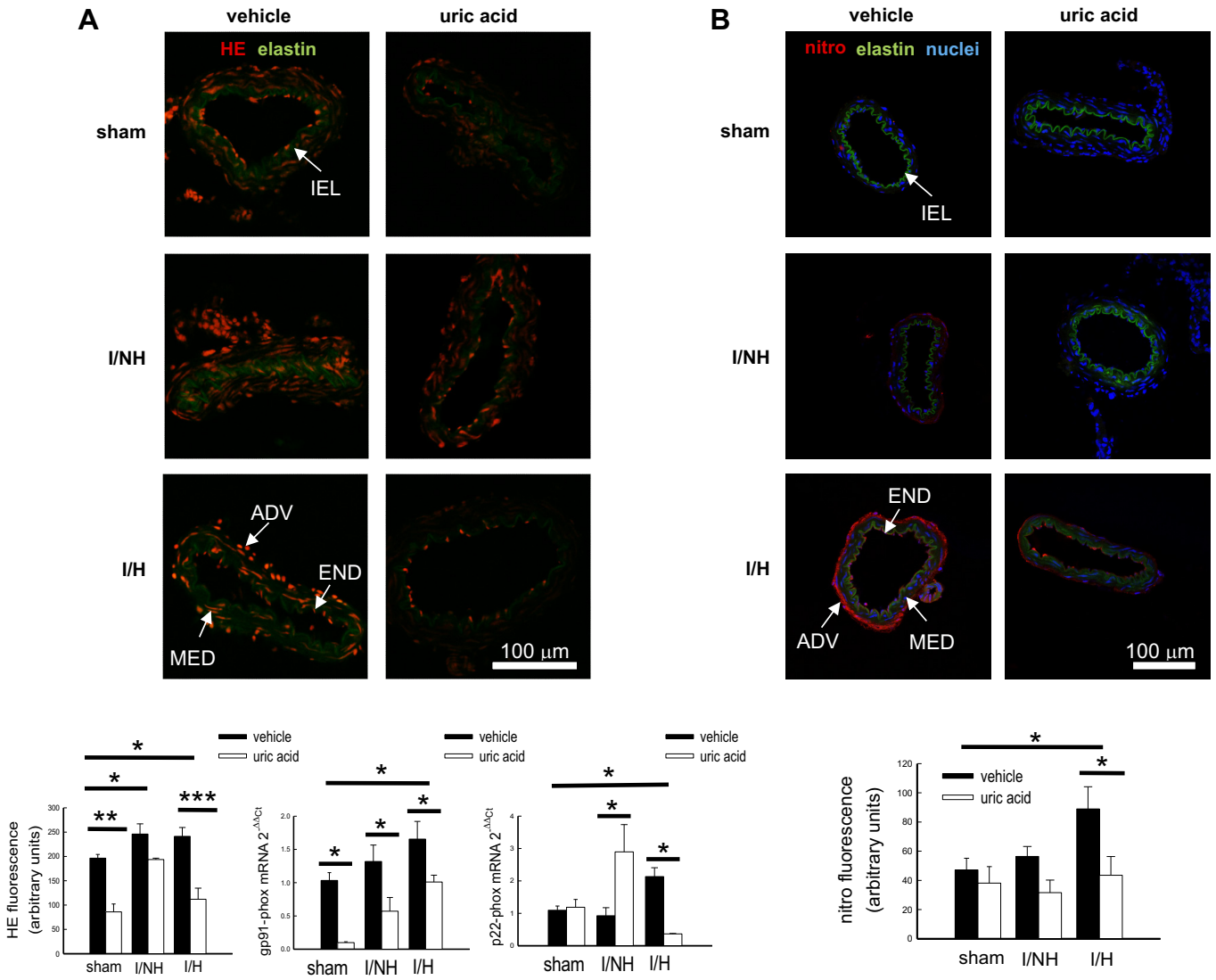

Fig. 5. Influence of uric acid treatment on oxidative stress and protein nitrotyrosination induced by ischemia-reperfusion in rat middle cerebral arteries. *A*: representative photomicrographs and quantification of fluorescence intensity of confocal microscopic artery sections labeled with the oxidative dye dihydroethidium, which produces a red fluorescence when oxidized to ethidium bromide by superoxide anion. Natural autofluorescence of elastin (green) is also shown. Comparative analysis of mRNA levels of the NAD(P)H oxidase subunit gp91^{phox} and p22^{phox} is also shown (*bottom*). mRNA levels are expressed as $2^{-\Delta\Delta C_t}$ using 18S as an internal control. *B*: representative photomicrographs and quantification of nitrotyrosine immunofluorescence of confocal microscopic artery sections. Immunofluorescence signal (red), natural autofluorescence of elastin (green), and nuclear staining (blue) are shown. HE, hydroethidine; Nitro, nitrotyrosine. Results are means ± SE from sham (vehicle: n = 7–10; uric acid: n = 4–5), I/NH (vehicle: n = 6–12; uric acid: n = 3–5), and I/H (vehicle: n = 5–8; uric acid: n = 3–7) rats. *$P < 0.05$, **$P < 0.01$, and ***$P < 0.001$ by 2-way ANOVA with Bonferroni's posttest.

was impaired in the MCA regardless of the status of protein nitrotyrosination 24 h after I/R, and UA treatment reduced protein nitrotyrosination without restoring the myogenic response in hyperemic rats. However, the myogenic tone of the MCA might suffer a long-lasting or irreversible impairment due to an early production of $ONOO^-$ as already suggested (14), which might not be restored by treatments administered later than 2 h after the onset of ischemia. Accordingly, a recent study demonstrated successful recovery of the myogenic response by $ONOO^-$ scavenging at reperfusion after shorter periods of ischemia (8).

Improving brain perfusion is essential to prevent neuronal death after ischemic stroke. UA infusion was associated with a passive lumen diameter expansion at 24 h. It has been described that nitrotyrosination of UA by $ONOO^-$ can form a product that can release NO (30). Even though circulating nitrite levels at 24 h after reperfusion in UA-treated hyperemic rats were low, we cannot exclude that a potential blood flow increase due, at least in part, to a UA-derived nitration/nitrosation product during reperfusion might contribute to the flow (shear stress)-induced outward remodeling (36). It is possible that the UA-induced luminal expansion of the MCA prevents the secondary hypoperfusion described to take place after reactive hyperemia (34).

In response to stress stimuli, such as overdistension or hypoxia, vascular adventitial cells (ACs) exhibit, among others, increases in adhesion proteins, secretion of chemokines and cytokines, and cell proliferation (31). Our group previously reported an increase in MCA AC number (AC hyperplasia) in rats after I/R, contributing to explain the increased external

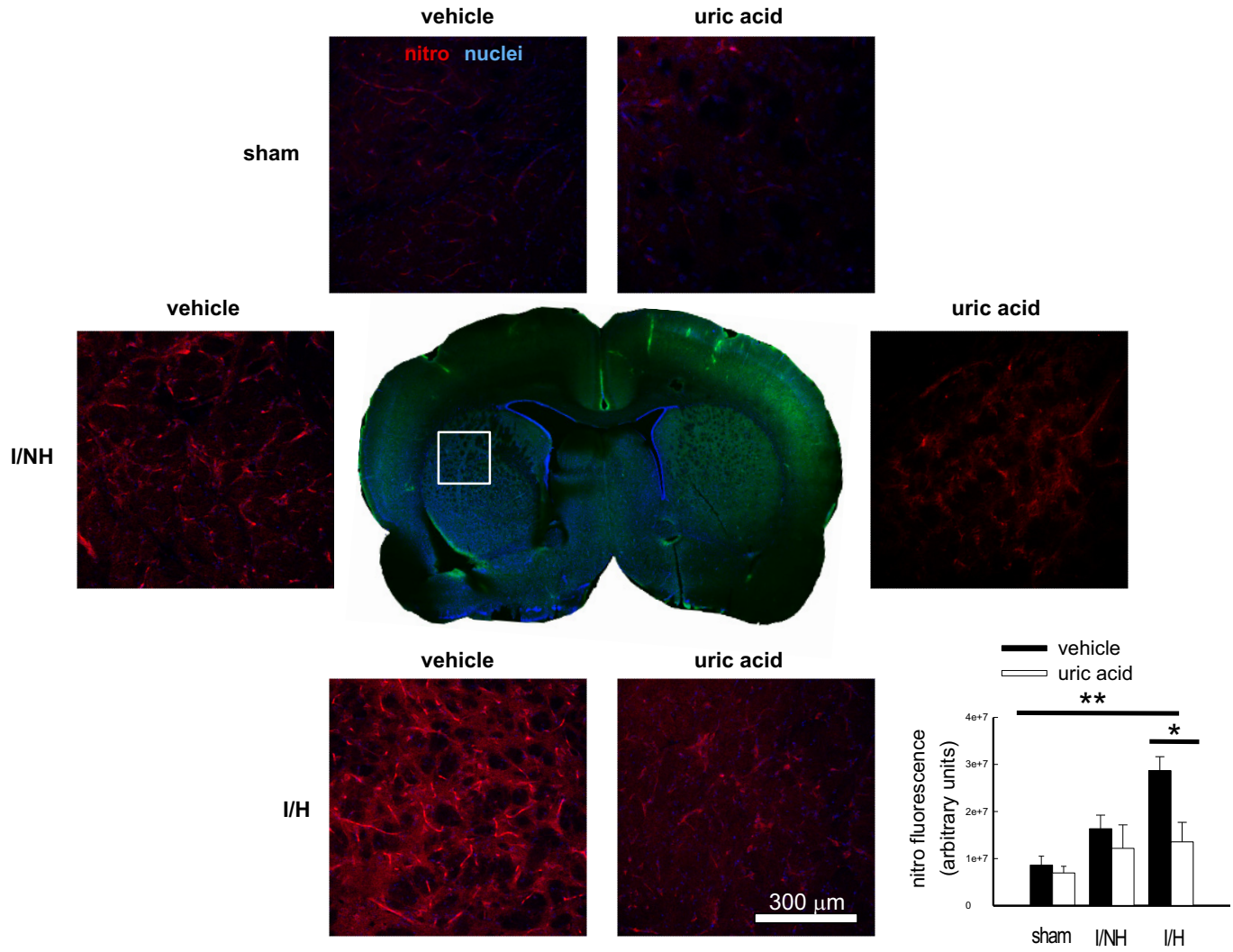

Fig. 6. Influence of uric acid treatment on rat brain protein nitrotyrosination induced by ischemia-reperfusion. Representative photomicrographs and quantification of nitrotyrosine immunofluorescence of close ups of the region of interest in the brain. Immunofluorescence signal (red) and nuclear staining (blue) are shown. Results are means ± SE from sham (vehicle: $n = 3$; uric acid: $n = 3$), I/NH (vehicle: $n = 3$; uric acid: $n = 3$), and I/H (vehicle: $n = 3$; uric acid: $n = 3$) rats. *$P < 0.05$ and **$P < 0.01$ by 2-way ANOVA with Bonferroni's posttest.

diameter and the subsequent wall thickening (15). Here we confirm those results and report that AC hyperplasia is a factor involved in MCA external diameter increase leading to hypertrophic remodeling in hyperemic rats. Vascular adventitia is considered an important source of ROS predominantly via NAD(P)H oxidase (31). Previous studies have suggested a relationship between hypertrophy and generation of free radical species in the rat MCA (3, 14). Although we detected

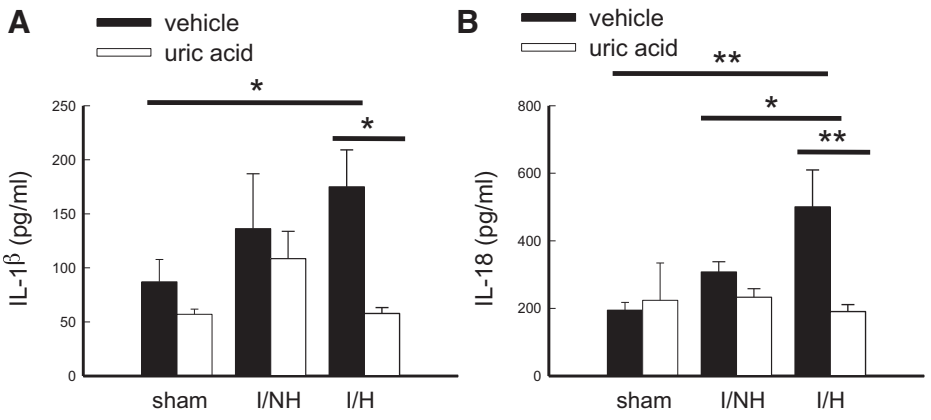

Fig. 7. Influence of uric acid treatment on plasma cytokines (pg/ml) after ischemia-reperfusion. IL, interleukin. Results are means ± SE from sham (vehicle: $n = 7$; uric acid: $n = 3$), I/NH (vehicle: $n = 7$; uric acid: $n = 7$), and I/H (vehicle: $n = 7$; uric acid: $n = 7$) rats. *$P < 0.05$ and **$P < 0.01$ by 2-way ANOVA with Bonferroni's posttest.

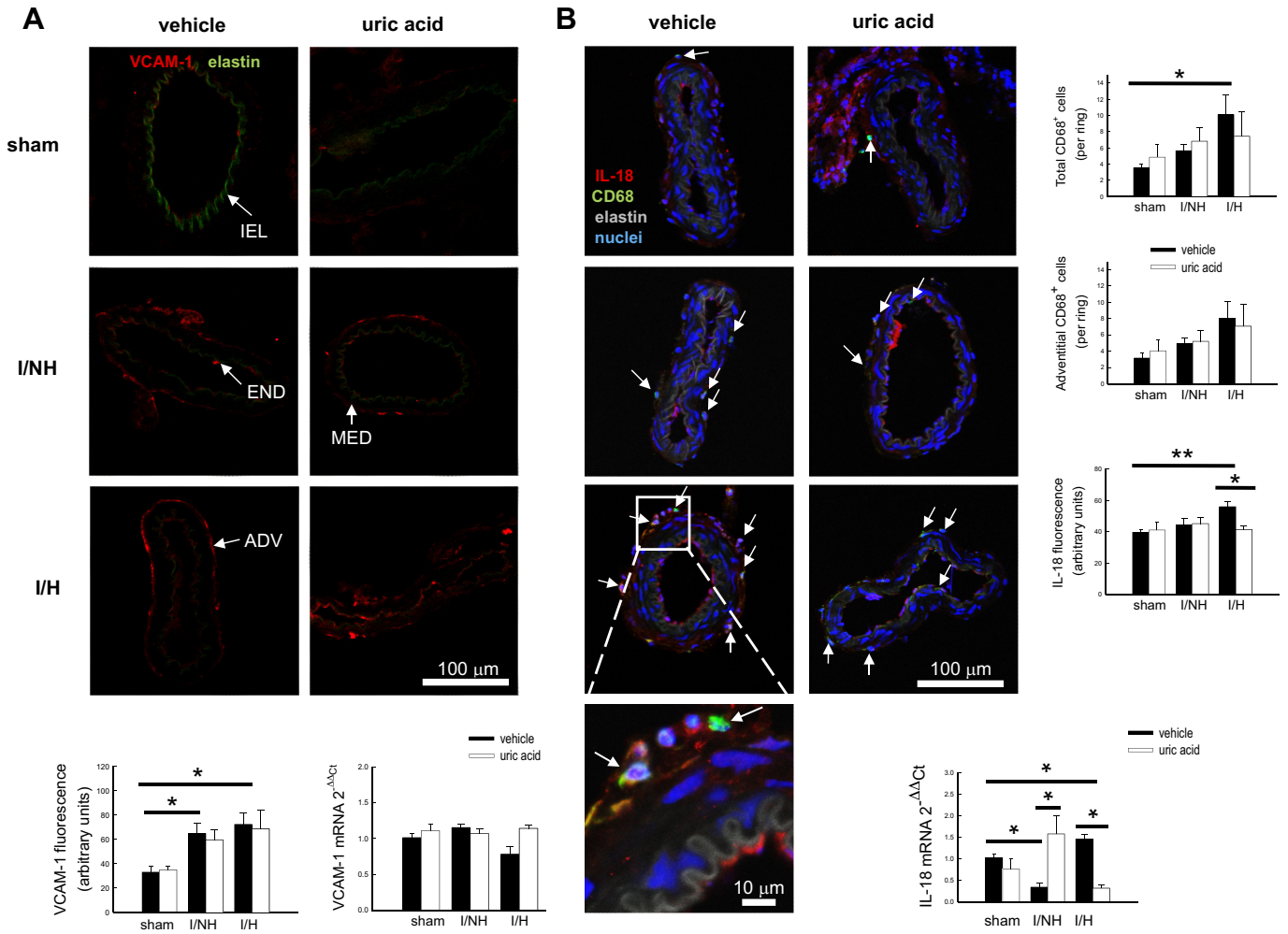

Fig. 8. Influence of uric acid treatment on inflammatory response induced by ischemia-reperfusion in rat middle cerebral arteries. Representative photomicrographs and quantification of vascular cell adhesion molecule-1 (VCAM-1; red) immunofluorescence (*A*) or IL-18 (red) and cluster of differentiation 68 (CD68; green) double immunofluorescence (*B*) of confocal microscopic artery sections. Natural autofluorescence of elastin (green or gray) and nuclear staining (blue) are shown. Representative examples of CD68-positive cells are indicated with arrows. Comparative analysis of mRNA levels of VCAM-1 (*A*) and IL-18 (*B*) are also shown. mRNA levels are expressed as $2^{-\Delta\Delta Ct}$ using 18S as the internal control. Results are means ± SE from sham (vehicle: $n = 4–7$; uric acid: $n = 4–5$), I/NH (vehicle: $n = 4–6$; uric acid: $n = 3–4$), and I/H (vehicle: $n = 3–5$; uric acid: $n = 3–6$) rats. $^*P < 0.05$ and $^{**}P < 0.01$ by 2-way ANOVA with Bonferroni's posttest.

similar ischemia-induced increases in $O_2^{\cdot-}$ formation, the MCA from hyperemic rats showed increased NAD(P)H oxidase subunit mRNA levels and augmented protein nitrotyrosination compared with nonhyperemic rats, suggesting that hyperemia is associated with exacerbated oxidative stress. UA antioxidant treatment diminished both oxidative stress and ERK1/2 activation and reduced AC proliferation, indicating a key role of oxidative stress in AC hyperplasia. ROS production by adventitial fibroblasts can promote the recruitment of inflammatory cells (25, 31), which in turn generate more ROS, magnifying the impact of oxidative stress (31). Hyperemia was associated with an increased presence of monocytes/macrophages ($CD68^+$ cells), mainly in the MCA adventitia, suggesting that increased adventitial oxidative stress in hyperemic animals could be involved in adventitial monocyte/macrophage recruitment.

Cerebral I/R triggers an inflammatory response that contributes to exacerbate brain damage. Initiation of the inflammatory response can involve the multiprotein complexes termed "inflammasomes" leading to release of proinflammatory cytokines (37). We detected increased levels of circulating IL-1β and IL-18 at 24 h in hyperemic compared with sham animals that were normalized by UA treatment. IL-18 expression was also increased in the MCA wall of hyperemic rats at 24 h, and this effect was prevented by UA treatment. Therefore, these results relate hyperemia with an oxidative stress-dependent cerebrovascular IL-18 accumulation, pointing to a role of IL-18 in early stage inflammation of the cerebral vasculature.

In summary, we demonstrate for the first time that MCA structural, but not myogenic, alterations observed after I/R are restricted to rats that manifest reactive hyperemia at early reperfusion. The underlying mechanism involves prominent oxidative stress, increased macrophage recruitment, and IL-18 accumulation in the MCA of hyperemic rats. This altered environment might favor AC proliferation contributing to MCA remodeling. We also show that exogenously administered UA exerts a more potent brain protective action in

Table 3. *Permeability in the parallel artificial membrane permeation-blood-brain barrier assay and predictive penetration in the CNS*

Compound	Bibliography Value	Experimental Values	CNS Prediction
Verapamil	16.0	27.9 ± 0.94	CNS^+
Testosterone	17.0	24.2 ± 0.79	CNS^+
Costicosterone	5.1	6.7 ± 0.22	CNS^+
Clonidine	5.3	6.5 ± 0.22	CNS^+
Ofloxacin	0.8	1.0 ± 0.03	CNS^-
Lomefloxacin	0.0	0.8 ± 0.02	CNS^-
Progesterone	9.3	16.8 ± 0.56	CNS^+
Promazine	8.8	13.8 ± 0.46	CNS^+
Imipramine	13.0	12.3 ± 0.45	CNS^+
Hidrocortisone	1.9	1.4 ± 0.05	CNS^-
Piroxicam	2.5	1.9 ± 0.06	CNS^-
Desipramine	12.0	17.8 ± 0.50	CNS^+
Cimetidine	0.0	0.7 ± 0.02	CNS^-
Norfloxacine	0.1	0.9 ± 0.06	CNS^-
Uric acid		0.2 ± 0.01	CNS^-

Results are means ± SE (10^{-6} cm/s) of $n = 3$ experiments. CNS, central nervous system.

hyperemic than in nonhyperemic rats, at least, by suppressing hyperemia-related MCA wall oxidative stress, inflammation, and hypertrophy and inducing MCA passive lumen diameter expansion. These results provide new insights into the mechanisms by which this compound exerts its protective actions against I/R-induced brain injury. The current data support the concept that UA exerts short-term vascular protection in young male rats. It will be necessary to validate these findings in female rats and in animals with comorbidities and to examine whether the potential UA benefits are sustained in the long term.

ACKNOWLEDGMENTS

We are grateful to Sofia Romeeva, Cristina Marsili, and Ferran Tarrés for the technical assistance and to the confocal microscopy core from the Universitat Autònoma de Barcelona.

GRANTS

The research was funded by grants from Ministerio de Ciencia e Innovación (SAF2010-19282), Generalitat de Catalunya (2009SGR-890), Laboratorios Almirall (2013), and Instituto Carlos III (FIS PI080176; CP06/00308; Red HERACLES RD12/0042/0006). Y. Onetti is a predoctoral fellow of the Ministerio de Educación y Ciencia.

DISCLOSURES

No conflicts of interest, financial or otherwise, are declared by the authors.

AUTHOR CONTRIBUTIONS

Author contributions: Y.O., A.P.D., B.P., R.C., and F.J.-A. performed experiments; Y.O., A.P.D., E.V., and F.J.-A. analyzed data; Y.O., A.P.D., B.P., E.V., and F.J.-A. prepared figures; Y.O. and F.J.-A. drafted manuscript; Y.O.,

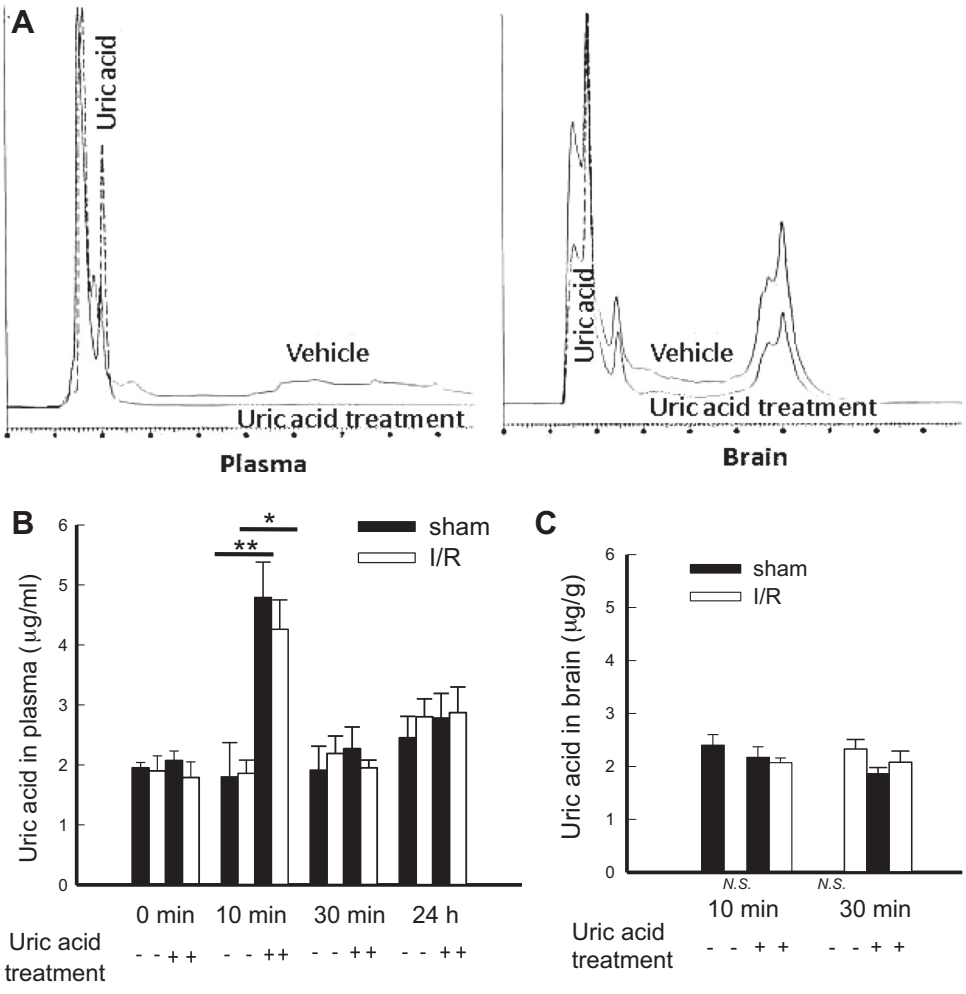

Fig. 9. Detection of uric acid in plasma (μg/ml) and brain (μg/g). The concentration of uric acid was quantified by HPLC using ultraviolet detection. Uric acid elutes from the column with 2-min retention time (*A*). The uric acid detection limit in plasma and brain samples was 10 ng/ml and 25 ng/g, respectively. *B*: plasma was studied at 0 min (before treatment), 10 min, 30 min (n = 3–4), and 24 h (n = 3–4) after iv uric acid administration. *C*: brain was studied at either 10 min (n = 3–4) or 30 min (n = 4–5). A similar endogenous uric acid signal was detected among groups in plasma and brain before exogenous administration. The highest plasma uric acid concentration was found at 10 min in both sham and ischemia-reperfusion (I/R) groups. No differences were detected in brain among groups at either time point. NS, not studied. Results are means ± SE from sham (vehicle: n = 3–4; uric acid: n = 3–7) and I/R (vehicle: n = 4; uric acid: n = 3–7) rats. *$P < 0.05$ and **$P < 0.01$ by 2-way ANOVA with Bonferroni's posttest.

A.P.D., B.P., R.C., A.C., A.M.P., E.V., and F.J.-A. approved final version of manuscript; A.C., A.M.P., E.V., and F.J.-A. edited and revised manuscript; A.M.P., E.V., and F.J.-A. interpreted results of experiments; E.V. and F.J.-A. conception and design of research.

REFERENCES

1. **Amaro S, Planas AM, Chamorro A.** Uric acid administration in patients with acute stroke: a novel approach to neuroprotection. *Expert Rev Neurother* 8: 259–270, 2008.
2. **Arribas SM, Hillier C, González C, McGrory S, Dominiczak AF, McGrath JC.** Cellular aspects of vascular remodeling in hypertension revealed by confocal microscopy. *Hypertension* 30: 1455–1464, 1997.
3. **Baumbach GL, Didion SP, Faraci FM.** Hypertrophy of cerebral arterioles in mice deficient in expression of the gene for CuZn superoxide dismutase. *Stroke* 37: 1850–1855, 2006.
4. **Beckman JS, Beckman TW, Chen J, Marshall PA, Freeman BA.** Apparent hydroxyl radical production by peroxynitrite: implications for endothelial injury from nitric oxide and superoxide. *Proc Natl Acad Sci USA* 87: 1620–1624, 1990.
5. **Chamorro A, Amaro S, Castellanos M, Segura T, Arenillas J, Martí-Fábregas, J, Gállego J, Krupinski J, Gomis M, Cánovas D, Carné X, Deulofeu R, Román LS, Oleaga L, Torres F, Planas AM; Investigators URICOICTUS.** Safety and efficacy of uric acid in patients with acute stroke (URICO-ICTUS): a randomised, double-blind phase 2b/3 trial. *Lancet Neurol* 13: 453–460, 2014.
6. **Cipolla MJ, Lessov N, Hammer ES, Curry AB.** Threshold duration of ischemia for myogenic tone in middle cerebral arteries: effect on vascular smooth muscle actin. *Stroke* 32: 1658–1664, 2001.
7. **Cipolla MJ, McCall AL, Lessov N, Porter JM.** Reperfusion decreases myogenic reactivity and alters middle cerebral artery function after focal cerebral ischemia in rats. *Stroke* 28: 176–180, 1997.
8. **Coucha M, Li W, Johnson MH, Fagan SC, Ergul A.** Protein nitration impairs the myogenic tone of rat middle cerebral arteries in both ischemic and nonischemic hemispheres after ischemic stroke. *Am J Physiol Heart Circ Physiol* 305: H1726–H1735, 2013.
9. **Di L, Kerns EH, Fan K, McConnell OJ, Carter GT.** High throughput artificial membrane permeability assay for blood-brain barrier. *Eur J Med Chem* 38: 223–232, 2003.
10. **Faraci FM, Heistad DD.** Regulation of large cerebral arteries and cerebral microvascular pressure. *Circ Res* 66: 8–17, 1990.
11. **Green LC, Wagner DA, Glogowski J, Skiper PL, Wishnock JS, Tannenbaum SR.** Analysis of nitrate, nitrite and [15N]nitrate in biological fluids. *Anal Biochem* 126: 131–138, 1982.
12. **Humphreys SA, Koss MC.** Role of nitric oxide in post-ischemic cerebral hyperemia in anesthetized rats. *Eur J Pharmacol* 347: 223–229, 1998.
13. **Jiang Z, Li C, Arrick DM, Yang S, Baluna AE, Sun H.** Role of nitric oxide synthases in early blood-brain barrier disruption following transient focal cerebral ischemia. *PLoS One* 9: e93134, 2014.
14. **Jiménez-Altayó F, Caracuel L, Pérez-Asensio FJ, Martínez-Revelles S, Messeguer A, Planas AM, Vila E.** Participation of oxidative stress on rat middle cerebral artery changes induced by focal cerebral ischemia: beneficial effects of 3,4-dihydro-6-hydroxy-7-methoxy-2,2-dimethyl-1(2H)-benzopyran (CR-6). *J Pharmacol Exp Ther* 331: 429–436, 2009.
15. **Jiménez-Altayó F, Martín A, Rojas S, Justicia C, Briones AM, Giraldo J, Planas AM, Vila E.** Transient middle cerebral artery occlusion causes different structural, mechanical, and myogenic alterations in normotensive and hypertensive rats. *Am J Physiol Heart Circ Physiol* 293: H628–H635, 2007.
16. **Kidwell CS, Saver JL, Mattiello J, Starkman S, Vinuela F, Duckwiler Gobin YP G, Jahan R, Vespa P, Villablanca JP, Liebeskind DS, Woods RP, Alger JR.** Diffusion-perfusion MRI characterization of post recanalization hyperperfusion in humans. *Neurology* 57: 2015–2021, 2001.
17. **Kim KM, Henderson GN, Ouyang X, Frye RF, Sautin YY, Feig DI, Johnson RJ.** A sensitive and specific liquid chromatography-tandem mass spectrometry method for the determination of intracellular and extracellular uric acid. *J Chromatogr B Analyt Technol Biomed Life Sci* 877: 2032–2038, 2009.
18. **Ma YH, Su N, Chao XD, Zhang YQ, Zhang L, Han Luo P F, Fei Z, Qu Y.** Thioredoxin-1 attenuates post-ischemic neuronal apoptosis via reducing oxidative/nitrative stress. *Neurochem Int* 60: 475–483, 2012.
19. **Maneen MJ, Hannah R, Vitullo L, DeLance N, Cipolla MJ.** Peroxynitrite diminishes myogenic activity and is associated with decreased vascular smooth muscle F-actin in rat posterior cerebral arteries. *Stroke* 37: 894–899, 2006.
20. **Mellander S.** Functional aspects of myogenic vascular control. *J Hypertens Suppl* 7: S21–S31, 1989.
21. **Novensa L, Selent J, Pastor M, Sandberg K, Heras M, Dantas AP.** Equine estrogens impair nitric oxide production and endothelial nitric oxide synthase transcription in human endothelial cells compared with the natural 17β-estradiol. *Hypertension* 56: 405–411, 2010.
22. **Palomares SM, Cipolla MJ.** Myogenic tone as a therapeutic target for ischemic stroke. *Curr Vasc Pharmacol* 12: 788–800, 2014.
23. **Pérez-Asensio FJ, de la Rosa X, Jiménez-Altayó F, Gorina R, Martínez E, Messeguer A, Vila E, Chamorro A, Planas AM.** Antioxidant CR-6 protects against reperfusion injury after a transient episode of focal brain ischemia in rats. *J Cereb Blood Flow Metab* 30: 638–652, 2010.
24. **Pires PW, Dams Ramos CM, Matin N, Dorrance AM.** The effects of hypertension on the cerebral circulation. *Am J Physiol Heart Circ Physiol* 304: H1598–H1614, 2013.
25. **Pires PW, Girgla SS, McClain JL, Kaminski NE, van Rooijen N, Dorrance AM.** Improvement in middle cerebral artery structure and endothelial function in stroke-prone spontaneously hypertensive rats after macrophage depletion. *Microcirculation* 20: 650–661, 2013.
26. **Pires PW, Girgla SS, Moreno G, McClain JL, Dorrance AM.** Tumor necrosis factor-α inhibition attenuates middle cerebral artery remodeling but increases cerebral ischemic damage in hypertensive rats. *Am J Physiol Heart Circ Physiol* 307: H658–H669, 2014.
27. **Planas AM, Traystman RJ.** Advances in translational medicine 2010. *Stroke* 42: 283–284, 2011.
28. **Romanos E, Planas AM, Amaro S, Chamorro A.** Uric acid reduces brain damage and improves the benefits of rt-PA in a rat model of thromboembolic stroke. *J Cereb Blood Flow Metab* 27: 14–20, 2007.
29. **Shi H, Liu KJ.** Cerebral tissue oxygenation and oxidative brain injury during ischemia and reperfusion. *Front Biosci* 12: 1318–1328, 2007.
30. **Skinner KA, White CR, Patel R, Tan S, Barnes S, Kirk M, Darley-Usmar V, Parks DA.** Nitrosation of uric acid by peroxynitrite. Formation of a vasoactive nitric oxide donor. *J Biol Chem* 273: 24491–24497, 1998.
31. **Stenmark KR, Yeager ME, El Kasmi KC, Nozik-Grayck E, Gerasimovskaya EV, Li M, Riddle SR, Frid MG.** The adventitia: essential regulator of vascular wall structure and function. *Annu Rev Physiol* 75: 23–47, 2013.
32. **Stoll G, Jander S, Schroeter M.** Inflammation and glial responses in ischemic brain lesions. *Prog Neurobiol* 56: 149–171, 1998.
33. **Tamura A, Asano T, Sano K.** Correlation between rCBF and histological changes following temporary middle cerebral artery occlusion. *Stroke* 11: 487–493, 1980.
34. **Traupe H, Kruse E, Heiss WD.** Reperfusion of focal ischemia of varying duration: postischemic hyper- and hypo-perfusion. *Stroke* 13: 615–622, 1982.
35. **Tsuchidate R, He QP, Smith ML, Siesjö BK.** Regional cerebral blood flow during and after 2 h of middle cerebral artery occlusion in the rat. *J Cereb Blood Flow Metab* 17: 1066–1073, 1997.
36. **Vessières E, Freidja ML, Loufrani L, Fassot C, Henrion D.** Flow (shear stress)-mediated remodeling of resistance arteries in diabetes. *Vascul Pharmacol* 57: 173–178, 2012.
37. **Walsh JG, Muruve DA, Power C.** Inflammasomes in the CNS. *Nat Rev Neurosci* 15: 84–97, 2014.
38. **Wang X, Tsuji K, Lee SR, Ning M, Furie KL, Buchan AM, Lo EH.** Mechanisms of hemorrhagic transformation after tissue plasminogen activator reperfusion therapy for ischemic stroke. *Stroke* 35, *Suppl* 1: 2726–2730, 2004.
39. **Yu ZF, Bruce-Keller AJ, Goodman Y, Mattson MP.** Uric acid protects neurons against excitotoxic and metabolic insults in cell culture, and against focal ischemic brain injury in vivo. *J Neurosci Res* 53: 613–625, 1998.